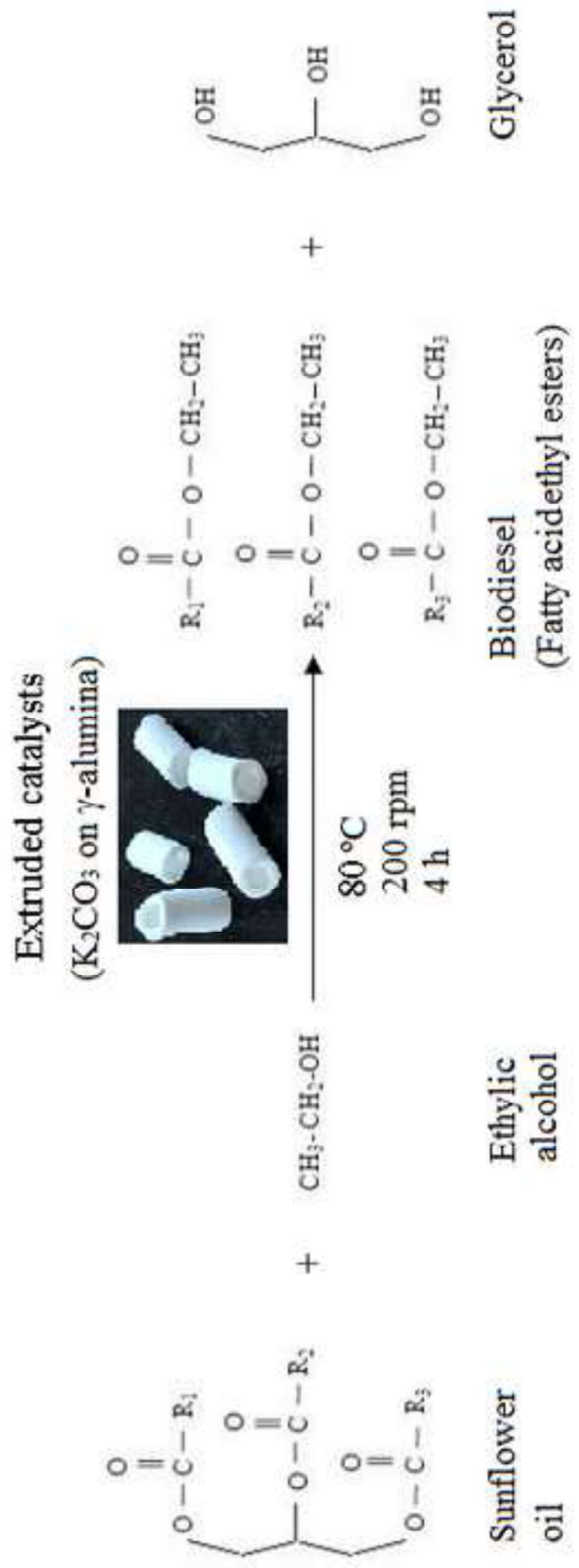


Highlights

- ✓ Extruded catalysts show efficient conversion of sunflower oil into biodiesel.
- ✓ The reaction achieved practically total conversion using 35%K₂CO₃/65%γ-Al₂O₃ at 2h.
- ✓ After transesterification high-quality biodiesel was attained according ASTM/EN specifications.

© 2018. This manuscript version is made available under the CC-BY-NC-ND 4.0 license <http://creativecommons.org/licenses/by-nc-nd/4.0/>



Biodiesel production from heterogeneous catalysts based K_2CO_3 supported on extruded $\gamma-Al_2O_3$

Euripedes G. Silveira Junior^a, Victor Haber Perez^{a*}, Inés Reyero^b, Ana Serrano-Lotina^c,
Oselys Rodriguez Justo^d

^aProcess Engineering Sector - Pilot Plant State University of the Northern of Rio de Janeiro, Rio de Janeiro, Brazil

^bDepartment of Applied Chemistry, Public University of Navarra, Campus of Arrosadía Pamplona, Spain

^cInstitute of Catalysis and Petrochemistry (CSIC) Campus of the Autonomous University of Madrid, Spain

^d*Environmental School, Estácio de Sá University, Campos dos Goytacazes. RJ, Brazil.*

*Corresponding Author:

Dr. Victor Haber Perez
Associate Professor
State University of Northern of Rio de Janeiro (UENF)
(CCTA)/ LTA - Processes Engineering Sector)
Av Alberto Lamego 2000
Pq California. Campos dos Goytacazes - RJ
Zip code: 28013-602. Brazil.
Phone. +55 (22) 27486085
Fax. +55 (22) 27397491
Cell. +55 (22) 997929553
E-mail: victorhaberperetz@gmail.com

Abstract

The biodiesel production from sunflower oil by ethanolic route using $K_2CO_3/\gamma-Al_2O_3$ with several shapes were studied. To prepare the catalysts, boehmite was extruded with the aid of a binder and different percentages of K_2CO_3 active phase (15 to 45%) impregnated on the supports for comparative purposes. **The transesterification reactions were carried out during 4h using 5 wt% of the catalyst and the effects of oil: alcohol molar ratio and temperature were investigated to improve biodiesel formation.** The best result (99.3% conversion) was obtained when 35% K_2CO_3 /65% $\gamma-Al_2O_3$ **hollow cylinder** catalyst was used at 80 °C and 1:12 oil: ethanol molar ratio, showing their potential as promising alternative to conventional homogeneous catalytic systems used for biodiesel production at industrial scale.

Keywords: Biodiesel, extruded catalysts, sunflower oil, ethanolic route

1. Introduction

The search for alternatives to mitigate global warming is nowadays one of most major global challenge. In this context, bioethanol, biobutanol, biodiesel, biogas (biomethane) and biofuels based on hydrogen and biomass are among the alternatives with great potential. Particularly, biodiesel, which is the focus of this work, is very attractive because it can be used in diesel engines without any modification and, moreover, can be produced by chemically and biochemically route. The world production of biodiesel in 2017 was 30.7 billion liters whose global ranking is led by United States of America (6.0×10^9 L), followed by Brazil (4.3×10^9 L), Germany (3.5×10^9 L) and Argentina (3.3×10^9 L), among others [1]. In Brasil, the commercial diesel/biodiesel blends containing 10% of biodiesel are mandatories as established by the National Energy Policy Council (CNPE) from the Brazilian Ministry of Mines and Energy. Basically, Its production at industrial scale is still carry out by chemical

transesterification using homogeneous alkaline catalyst such as KOH or NaOH or their corresponding alkoxide (CH_3ONa^+ or CH_3OK^+) and methanol as reactant alcohol [2]. This conventional process for biodiesel production, including its advantages and drawbacks has been extensively discussed [3-5]. However, the main challenges are still focused on the main following aspects: a) use of the non-edible oils as feedstocks; b) new applications for glycerol and c) technological improvement to reduce its production cost, including development of the new processes and unexpensive heterogeneous catalysts, among others.

In this context, an extensive research activity about the use heterogeneous catalysts as alternative to the conventional homogeneous catalysts has been observed [6-12]. In these cases, are required reaction temperature and molar ratios of oil: alcohol comparatively higher, however, soap production is avoided and catalysts can be easily recovered and reused in several reaction cycles, resulting, consequently, in processes with lower environmental impact.

Several solid catalysts, such as basic derivatives [13-15], acids [16, 17] and bifunctional systems [18, 19] have been evaluated, as well as, enzymatic derivatives, which have shown excellent performance despite the high commercial cost of the purified enzymes[20, 21]. There is still no consensus, however, as to whether alkaline catalysts are a better choice than acid in terms of reaction rate and biodiesel productivity. One disadvantage of the use of a solid catalyst is the formation multiphasic system, which leads to diffusion limitations that decrease the reaction rate [2, 22].

Also, instead of the powder catalysts, the extruded heterogeneous catalysts [23-29] present a great potential and are very attractive due to their conformed structure with different geometrical shapes which can create a macroporous material with mesopores connecting clusters of catalyst supports. Also, the extruded larger catalysts present good

mechanical properties and allow for easier recovery from reactional medium for regeneration resulting in excellent catalysts for several applications.

On the other hand, after a careful analysis of studies on a wide variety of heterogeneous catalytic derivatives reported in the literature [10, 11, 30-37] found a family of catalysts based on potassium precursors [30-37]. Among them, $K_2CO_3/\gamma-Al_2O_3$ in powder form was attractive because of its easy preparation and low cost [30, 33]. This powder catalyst has already been explored in the production of biodiesel, even if, by methylic route and using several feedstocks, with relatively good performance. However, depending on the reaction conditions, powder catalysts commonly present agglomeration problems that affect its catalytic activity. Thus, the aim of this work was to evaluate extruded catalysts based on $K_2CO_3/\gamma-Al_2O_3$, constituted by a channel with cylindrical geometry (hollow cylinder), in order to verify their potential in the ethanolic biodiesel production by chemical transesterification.

2. Materials and Methods

2.1 Materials

The used feedstock for biodiesel production was commercial sunflower oil. A mixture C4-C24 of fatty acid ethyl esters (FAEEs) was used as standard for biodiesel characterization (SUPELCO). Boehmite (PURAL SB SASOL containing 85% of Al_2O_3) was used as γ -alumina precursor and urea as temporary binder was used for the extrusion. Potassium carbonate (SCHARLAU) was used as active phase component and ethanol P.A. (SCHARLAU) was used as reagent alcohol.

2.2 Experimental methods

2.2.1 Procedure for support preparation

For comparative purpose three support with different shapes were evaluated: 1) boehmite powder; 2) boehmite hollow cylinder and 3) boehmite solid cylinder. In the

first case was used just boehmite as presented in its commercial form and calcinated at 500 °C for 4 h.

For the second and third cases, the materials used to prepare the support were boehmite (1625.70 g), temporary binder (151.25 g) and water (250 g). In order to extrude the boehmite, 4 process steps were necessary, being: a) mass formation; b) extrusion; c) drying (essential to avoid cracking in the extruded catalysts) and d) calcination. Firstly, the materials were mixed in a mechanical kneading machine (model R-02E orbital kneader model, from EIRICH, Germany) until homogeneity was reached. Then, water was added until achieving a good plasticity. The mixture was then mechanically mixed for 5 min and kept isolated at room temperature overnight. Then, after overnight the mechanical extrusion was performed in a Bonnot extruder (2209 model, form Bonnot Company, USA) at 6 rpm to obtain hollow cylindrical shapes of 5 mm of external and 2 mm internal diameter and solid cylinders of 1.83 mm of diameter, using a Cone Drive Transverse (Model SHU-7500C-BJ). The extrudates were dried for two days at room temperature and finally calcined in the muffle furnace at 500°C for 4h resulting in γ - Al_2O_3 structures.

2.2.2 Procedure for catalysts preparation

The catalysts were prepared by K_2CO_3 equilibrium impregnation on the hollow and solid cylinder supports using 15, 25, 35 and 45 % of K_2CO_3 respect to the support mass, during 1 h at 10 rpm. However, previously pore volume of the calcined supports were determined as $0.774 \text{ cm}^3 \cdot \text{g}^{-1}$ to estimate the active phase requested for impregnation procedure. For powder catalysts K_2CO_3 was incorporated on the supports by insipient impregnation. Finally, in all cases, the catalysts were calcined in the muffle furnace at 500°C for 4h.

2.2.3 Procedure for biodiesel production

The biodiesel production was carried out by chemical transesterification through ethanolic route using sunflower oil as substrate and using essentially K_2CO_3 supported on $\gamma-Al_2O_3$ with hollow cylindrical shapes as catalyst. In each experiment 5% mass of catalyst in relation to oil mass was used, whereas oil: alcohol molar ratio was varied: 1: 6, 1: 9 and 1: 12. The reactions were conducted in a glass jacketed reactor coupled to thermostatic bath to adjust the reactor temperature at 80 °C and under continuous agitation (200 rpm) during 4h reactional time. Then, the reaction was stopped and the biodiesel was purified as described previously by Silveira-Junior et al. [38] for further characterization. **Experiments were carried out in triplicate.** Powder and solid cylinder catalysts were just used for comparative purpose during diffusional limitation studies.

2.3 Analytical methods

2.3.1 Thermogravimetric analysis (TG/DTG)

Simultaneous thermogravimetric and differential thermal analyses (TGA-DTA) of catalysts were carried out in a flowing air atmosphere using an analyzer equipped with a gas cell (**STA 6000 model from PerkinElmer, USA**). Around 30 mg of sample were placed in a Pt/Rh crucible and heated up to 950°C with a heating rate of 10 °C/ min.

2.3.2 Mechanical strength

The mechanical strength of the catalysts was measured in terms of burst pressure using a dynamometer (**LTMC model from CHATILLON, USA**) according ASTM D 4179/2011. The tests consisted on determining the pressure needed to be applied on the external surface of the catalyst to cause its rupture.

2.3.3 Scanning Electron Microscopy (SEM)

SEM micrographs of the catalyst was obtained on a scanning electron microscope HITACHI (**TM1000 Tabletop Microscope model from HITACHI, Japan**). The procedure for preparing the materials for analysis consisted of depositing a portion of

the solid onto a carbon adhesive tape affixed to the sample holder. The micrographs were obtained with magnifications ranging from 100 to 3000 \times .

2.3.4 X-Ray diffraction

Analysis of the powder (support and/or catalysts) obtained by previous milling was performed by X-ray diffractometry (XRD, X'Pert PRO Theta/2theta from PANalytical, The Netherlands). The patterns were recorded over the angular range of 5–70° (2 θ) with a step size of 0.0334° and a time per step of 100 seconds, using Cu K α radiation ($\lambda = 0.154056$ nm) with a working voltage and current of 40 kV and 100 mA, respectively.

2.3.5 Textural characterization

Specific surface area data were calculated from nitrogen adsorption/desorption isotherms obtained at 196 °C in an ASAP apparatus (2420 model from Micromeritics Instrument Corp., USA), after application of the BET equation [39, 40].

2.3.6 Chemisorption analysis (CO₂- TPD)

Chemisorption analysis was carried out through the temperature-programmed desorption profiles of CO₂ (CO₂ - TPD) using apparatus equipped with a mass detector (AutoChem II 2920 V4.01 model from Micromeritics Instrument Corp., USA). Before the CO₂-TPD experiment, samples (0.2000 g) were treated in situ in a helium flow, heated to 200 °C at 10 °C/min and maintained for 30 min. The samples were then exposed to CO₂ at an initial temperature of 40 °C and with a ramp of 10 °C/min for 60 minutes and then heated to 500 °C at 10 °C/min under a Helium flow while it was monitoring the desorption of CO₂.

2.3.7 Gas chromatography (GC)

The formed biodiesel was monitored by gas chromatography (430-GC model from Bruker, Germany). The injector and detector temperatures were set at 250 °C. Helium

was used as the carrier gas with a flow of 312.3 mL/min of entrainment gas at a linear velocity of 62.0 cm/min. The column temperature was kept at 50°C for 1 min, heated to 180 °C at 15°C/min, then to 300 °C at 7 °C/min and maintained constant for 10 min. The detector temperature was 250 °C and the chromatographic column used was a Bruker BR 5 MS (30m×0.25mm×0.25um) with 5% diphenyl and 95% dimethyl polysiloxane composition. Identification and quantification of formed biodiesel was carried out according to the calibration curve prepared using FAEEs (referent to the fatty acids contained in the sunflower oil) at four concentrations and ethyl decanoate as internal standard (Sigma-Aldrich).

2.3.8 Physicochemical analysis of biodiesel using standard methods

Physicochemical analyses were carried out to evaluate the biodiesel quality according to standard **specifications** (US Standard - ASTM D6751 and European Standard - EN 14213), **considering particularly the following properties:** specific gravity (ASTM D1298), kinematic viscosity (ASTM D445), acid number (ASTM D664) and iodine index (EN 14111).

3. Results and discussion

3.1 Catalyst characterization

3.1.1 Thermogravimetric analysis of extruded support/ catalysts

Figure 1 shows the results of thermogravimetric analysis (TGA-DTG) of boehmite (Fig. 1a) and the active phase K_2CO_3 (Fig. 1b) between the temperature ranges of 30 and 950 °C. A thermogravimetric analysis (TGA-DTG) of boehmite is interesting to evaluate the most adequate calcination temperature for the extruded support preparation, in order to obtain the gamma phase of alumina and the complete elimination of the binder. As can be observed in the case of boehmite, between the temperature ranges of 50 and 200 °C, there is a loss of mass that is attributed to the surface water of its structure. While in the

temperature ranges between 400 and 500 °C the loss of OH groups occur and consequently there is a phase change from boehmite to γ -alumina. After 500 °C, the material does not change. In this case, 500 °C may be considered as the calcination temperature sufficient for the preparation of the carrier without the presence of the additive binder.

On the other hand, Figure 1b shows the TGA-DTG curve of the active phase (K_2CO_3) which revealed that up to 800 °C this still remains in its integral form. But, at temperature values above this material can result in K_2O . This fact is in agreement with the literature, which reports the decomposition of potassium carbonate around 850 to 890 °C [35, 41].

Figure 1 here

3.1.2 Morphological and mechanical strength of extruded support/ catalysts

Table 1 shows the mechanical strength values for hollow cylindrical shapes. This test is important to predict the resistance to breaking of these catalysts during the transesterification reactions. Normally the rupture of these systems can occur due to collisions between the catalysts or even the impact of these materials with the blade stirrers or the reactor walls. The tests were performed by dynamometry, which consists of measuring the mechanical resistance against a radial compression exerted on the material until its rupture (ASTM D 4179/2011).

Table 1 here

As can be observed in Table 1, the mechanical strength values were different, being higher in the catalysts with a composition of 35% of K_2CO_3 , which presented practically double (2.75 kgf/cm) in comparison with the other catalysts. This behavior can be attributed to a better distribution of the active phase component on the surface of the support, thus contributing to the formation of a more resistant structure.

3.1.3 XRD analysis of the extruded support/ catalysts

Figure 2 shows the results referent to the XRD curves for both, support and catalyst. The peaks appeared at 37° , 46° and 67° can be attributed to $\gamma\text{-Al}_2\text{O}_3$ (Wang et al., 2016). The presence of the active phase in the support can be validated by the formation of a diffraction peak formed at $2\theta = 32^\circ$ after the impregnation step which increases with the increase of the K_2CO_3 composition in the support.

According Wang et al. [41], when the loading amount of K_2CO_3 closely matches the amount of surface hydroxy groups, an optimum interaction between active phase and support results in the $\text{KAl(OH)}_2\text{CO}_3$ phase is reached, especially when the mixture between active phase and support is wet, as is the case here in question. Higher loading amounts will hinder the dispersion of potassium and lead to agglomeration of bulk carbonate.

Figure 2 here

3.1.4 Textural properties of extruded support/ catalyst

The textural properties for both, extruded support and catalysts are shown in Table 2. The extruded support and catalysts presented a Type IV isotherm, with a well-defined plateau at high relative pressure and narrow hysteresis loop on desorption after treatment at 500°C (calcination temperature). The Type IV character of these materials allowed an accurate assessment of the mesoporosity by converting the volume adsorbed at relative pressures $p/p_0 = 0.98$ on the desorption curve to a liquid volume, assuming the liquid density of nitrogen to be 0.808 g/cm^3 . Thus, at 500°C the calculated mesopore volumes were $0.55 \text{ cm}^3/\text{g}$ with a specific area of the $209 \text{ m}^2/\text{g}$ and pore size of the 9.8 nm .

Regarding the catalysts, it is observed that the specific area and the volume of pores decrease as the concentration of K_2CO_3 increases, and this is because the pores of the

support are filled with the active phase compound, consequently reducing the area and pore volume.

Table 2 here

3.1.5 CO₂-TPD analysis of extruded catalysts

In order to evaluate the strength and proportion of the different basic sites of the catalysts under study, programmed thermal desorption experiments of CO₂ (TPD-CO₂) were carried out. Table 3 shows the values concerning the total amount of CO₂ desorbed (mmol/g) and also the basic sites density (mmol/m²) as a function of the CO₂ desorption temperature. This type of analysis assumes that at the highest desorption temperatures greater catalyst basicity is attained because the temperature at which the CO₂ is desorbed from the catalysts reflects the strength of the surface bond, but resulting in peaks that can be correlated to three different types of active sites, e.g., weak, medium and strong sites which can be identified as follow: Strength of the basic sites: weak sites (CO₂ desorption below 160 °C); medium sites (CO₂ desorption between 160 and 400 °C) and strong sites (CO₂ desorption above 400 °C). Then, according to the attained desorption temperature, in all cases, were observed medium strength of the basic sites.

Table 3 also shows the basicity of K₂CO₃/γ-Al₂O₃ samples as a function of the active phase loading (from 15 to 45 wt% K₂CO₃). When the amount of loaded active phase increased from 15 to 35 wt%, the total density of basic sites was increased from 0.028 up to 0.070 mmol/m² reaching the maximum value for 35 wt% K₂CO₃. However, increase for 45 wt% K₂CO₃ resulted in decreased of the basicity. In fact, as can be observed in Table 3, for all catalysts two peak desorption were observed except for catalyst containing 45wt% active phase that presented just one desorption peak. When are correlate these behaviors with the catalytic performance of the different catalysts is clearly verified a drop in the biodiesel conversion (Fig. 5). Probably, this behavior can

be due to the undesirable coverage of basic sites on the catalyst surface by the excessive amount of K_2CO_3 .

This fact can also be explained based on the work of Wang et al. [41] who reported that the dispersion of the potassium salt in alumina depends on the potassium content in the composite. The authors consider that many defects observed in the alumina structure result in the dehydration of the OH groups of the surface, after the calcination. In this way, the dispersion of the active phase occurs by the incorporation of cations in these places through a strong interaction between support and active phase. Thus, if the amount of potassium salt coincides with the amount of OH on the support surface, an optimum interaction will occur, resulting in $KAl(OH)_2CO_3$ stoichiometric formation. When the potassium salt load is higher than the number of available sites, its dispersion will not be efficient and the result will be the agglomeration of carbonate crystals.

Table 3 here

3.1.6 Surface analysis of the extruded catalyst by SEM

Figure 3 shows the micrograph referent to $35\%K_2CO_3/\gamma-Al_2O_3$ catalyst from SEM analysis. It is noted the formation of well-distributed K_2CO_3 agglomerates on the support surface, corresponding to 49.8% according to EDS results.

Figure 3 here

3.2 Biodiesel production by extruded catalysts

3.2.1 Effect of the molar ratio oil: alcohol on the biodiesel production

The results of the effect of the oil: ethanol molar ratio on the biodiesel production are shown in Fig. 4. The experiments were carried out using a catalyst containing $35\%K_2CO_3/65\%\gamma-Al_2O_3$. According to the attained results, an increase in oil: ethanol molar ratio lead to an increase in the biodiesel yield. At 1:12 molar ratio, the biodiesel

yield was around 99 % at the reaction end (4 h). In addition, highest productivity (0.50 g/g h of biodiesel) was attained at 2h reaction time when 1:12 was also used (Table 4).

[Figure 4 here](#)

[Table 4 here](#)

The influence of the oil: alcohol molar ratio on heterogeneous catalysis is one of the factors that most affect: the conversion, the reaction yield, the production cost and the biodiesel purity [42, 43]. **The stoichiometric oil: alcohol molar ratio for biodiesel production is 1:3. However, larger molar ratios are conveniently used to change the reaction equilibrium toward biodiesel production.** In addition, the three-phase formation (oil, alcohol and catalyst) at the reaction beginning may restrict the contact between the reactive mixtures, in which case the excess alcohol in the reaction minimizes this problem. Also, co-solvents such as tetrahydrofuran [44], diethyl ether [45], acetone [46], n-hexane [47, 48], propane [49] have been used to enhance the miscibility of oil and alcohol and reaction rate of the transesterification.

3.2.2 Effect of the active phase loading on the biodiesel production

Figure 5 shows the reaction kinetics of sunflower biodiesel formation with the catalysts prepared by different K_2CO_3 load (15, 25, 35 and 45 %) relative to the $\gamma-Al_2O_3$ extruded support mass. According to the obtained results was verified that catalytic activity depends of its **basic strength**. In fact, catalysts with 15 and 25 % of K_2CO_3 were not efficient since attained just 78 and 76 % respectively. The catalyst with 35 % of K_2CO_3 showed the best performance, reaching 97 % and 0.51 g/g.h of yield and productivity (Table 5), respectively, at 2 h of reaction and practically reaching full yield at the transesterification end. While, increase of the catalyst loading to 45 % K_2CO_3 resulted in a poor catalytic performance (around 88 %) comparatively with last case. Probably,

this behavior can be explained by undesirable K_2CO_3 agglomeration on the support surface during the impregnation procedure.

[Figure 5 here](#)

[Table 5 here](#)

Similar results were attained by Xie et al. [50] which evaluated the effect of KI loading in ranging from 15 to 40 wt.% on the preparation of different KI/ Al_2O_3 catalysts samples in the soybean and methanol transesterification reactions. When loading amount of KI was raised from 15 to 35 wt.%, conversion increases, reaching 87.4 % conversions. However, when the amount of loaded KI was above 35 wt.%, the conversion was decreased. They related the lower activity with the covering of basic sites with the KI excess.

3.2.3 Effect of the catalyst shapes on the biodiesel yield

Since the 35% K_2CO_3 / γ - Al_2O_3 catalyst showed the best catalytic performance, the effect of the shape of the catalyst was conveniently over the biodiesel yield during the transesterification at the same reactional condition (Fig. 6), i.e., 80 °C, 1:12 oil: ethanol molar ratio and 200 rpm. Thus, three different catalytic shapes were considered for comparative purpose: 1) solid cylinder with 1.83 mm of diameter \times 5 mm length and 2) hollow cylindrical with 2 mm internal diameter \times 5 mm external diameter \times 5 mm length and 3) powder containing particles with 30 μ m. According to the attained results (Fig. 6), diffusional limitations were detected depending on the shape of the catalyst. The best performance was observed with the catalyst with a hollow cylindrical shape since there was a reduction of the catalytic activity when, both, powder and solid cylinder shape was evaluated.

Regarding to the powder catalyst, the biodiesel conversion at the beginning was higher, but after 60 min it was lower than the hollow cylinder shape. The decrease of the

activity can be related to the agglomeration of the small fine particles [2]. While, for the solid cylinder, porosimetry characterization indicated a lower macroporosity in this catalyst when compared with the hollow cylinder. Then, upon decreasing the catalyst porosity, the diffusion of the chemicals (oil, ethanol and biodiesel) on the surface or inside the pores can be reduced result in an undesirable diffusional limitation.

Figure 6 here

The Table 6 show some studies reported in the literature with catalysts prepared in different forms, i.e., including, both, powder and extruded for **biodiesel production**. **Comparatively, the prepared catalyst in our study presented a satisfactory performance**, catalyzing the biodiesel formation with high conversion rate under moderate reaction conditions respect to the powder catalysts showed in Table 6. **Powder catalysts present great difficult to be separated from a viscous reaction media**. Furthermore, an important aspect that should be considered is about particles sizes of the powder catalysts that are normally very fine and consequently, can form undesirable agglomeration in the reactional medium, thus affecting their catalytic performance [2]. **Besides the factors described above, the satisfactory performance of the catalyst prepared in our work can be attributed to its conformation with hollow cylinder geometry which favors a low pressure drop and a high geometric surface, thus attenuating the diffusional limitations observed in relation to the others catalysts presented in this study.**

Table 6 here

3.2.4 Biodiesel production study under different reaction temperatures

Figure 7 shows the biodiesel yield in reactions conducted at temperatures of 60, 70 and 80 °C. As can be observed when the reaction was conducted at temperature near the boiling point of ethanol, the yield of the reaction was better, achieving 97% conversion at 2h reaction, while that at temperature of 60 and 70 °C, reaction occurs more slowly,

requiring 4 hours to obtain the total conversion. Reaction temperatures below to the alcohol boiling point are attractive to avoid evaporation and alcohol losses [51]. Similar results were attained by Korkut and Bayramoglu [13] which evaluated the catalytic performance of CaO and dolomite in the transesterification of canola oil by ultrasound. The authors also reported that reaction temperature near the boiling point ensures a high biodiesel yield.

Figure 7 here

3.2.5 Physico-chemical properties of produced biodiesel

Table 7 shows the attained results referent to physico-chemical characterization of the sunflower biodiesel under study. Thus, its quality was confirmed by density, kinematic viscosity, acid number and iodine value properties whose values were in accordance with Brazilian standard specifications corroborating the potential of the catalysts under study.

Table 7 here

4. Conclusions

Several extruded catalysts based on K_2CO_3 on $\gamma-Al_2O_3$ were prepared by the active phase impregnation on the support to catalyze the biodiesel formation by transesterification with high conversion rate under moderate reaction conditions. The best results were obtained when 35% of K_2CO_3 was impregnated in the support and used as a catalyst in the transesterification reaction, reaching a yield and productivity in ethanolic biodiesel around 99 % and 0.5 g/g. respectively, at the reaction end. According to the attained results this developed extruded catalyst can be considered as an attractive alternative respect to the homogeneous catalysts for biodiesel production.

This technology could be economically viable at industrial scale; however, future works must be carried out to explore this question.

Acknowledgements

We are grateful to the Program of the Madrid Community AlcCones, S2013/MAE-2985, and to the Brazilian agencies: Carlos Chagas Filho Research Foundation of the Rio de Janeiro State (FAPERJ) (Process no. E-26/210.508/2014) and The National Council for Scientific and Technological Development (CNPq) (process no. 165577/2013-14 and 311942/2015-6) for the financial support.

References

- [1] REN21, Renewables 2018 Global Status Report. (Paris: REN21 Secretariat). ISBN. 978-3-9818911-3-3., in, 2018.
- [2] V.H. Perez, E.G. Silveira-Junior, D.C. Cubides, G.F. David, O.R. Justo, M.P.P. Castro, M.S. Sthel, H.F. de Castro, Trends in Biodiesel Production: Present Status and Future Directions. , in: S.S. da Silva, A.K. Chandel (Eds.) Biofuels in Brazil., Springer, 2014, pp. 281-302.
- [3] M.R. Avhad, J.M. Marchetti, A review on recent advancement in catalytic materials for biodiesel production, Renewable and Sustainable Energy Reviews, 50 (2015) 696-718.
- [4] A. Galadima, O. Muraza, Biodiesel production from algae by using heterogeneous catalysts: A critical review, Energy, 78 (2014) 72-83.
- [5] K. Neumann, K. Werth, A. Martín, A. Górak, Biodiesel production from waste cooking oils through esterification: Catalyst screening, chemical equilibrium and reaction kinetics, Chemical Engineering Research and Design, 107 (2016) 52-62.
- [6] A.P.S. Chouhan, A.K. Sarma, Modern heterogeneous catalysts for biodiesel production: A comprehensive review, Renewable and Sustainable Energy Reviews, 15 (2011) 4378-4399.

- [7] M. Kouzu, J.-s. Hidaka, Transesterification of vegetable oil into biodiesel catalyzed by CaO: A review, *Fuel*, 93 (2012) 1-12.
- [8] S. Mostafa Hosseini Asl, A. Ghadi, M. Sharifzadeh Baei, H. Javadian, M. Maghsudi, H. Kazemian, Porous catalysts fabricated from coal fly ash as cost-effective alternatives for industrial applications: A review, *Fuel*, 217 (2018) 320-342.
- [9] R. Shan, L. Lu, Y. Shi, H. Yuan, J. Shi, Catalysts from renewable resources for biodiesel production, *Energy Conversion and Management*, 178 (2018) 277-289.
- [10] S. Sharma, V. Saxena, A. Baranwal, P. Chandra, L.M. Pandey, Engineered nanoporous materials mediated heterogeneous catalysts and their implications in biodiesel production, *Materials Science for Energy Technologies*, 1 (2018) 11-21.
- [11] Y.C. Sharma, B. Singh, J. Korstad, Latest developments on application of heterogeneous basic catalysts for an efficient and eco friendly synthesis of biodiesel: A review, *Fuel*, 90 (2011) 1309-1324.
- [12] A.S. Yusuff, O.D. Adeniji, M. Olutoye, U.G. Akpan, A Review on Application of Heterogeneous Catalyst in the Production of Biodiesel from Vegetable Oils. , *Journal of Applied Science & Process Engineering*, 4 (2017) 142-157.
- [13] I. Korkut, M. Bayramoglu, Selection of catalyst and reaction conditions for ultrasound assisted biodiesel production from canola oil, *Renewable Energy*, 116 (2018) 543-551.
- [14] M. Kouzu, T. Kasuno, M. Tajika, S. Yamanaka, J. Hidaka, Active phase of calcium oxide used as solid base catalyst for transesterification of soybean oil with refluxing methanol, *Applied Catalysis A: General*, 334 (2008) 357-365.
- [15] I. Reyero, G. Arzamendi, L.M. Gandía, Heterogenization of the biodiesel synthesis catalysis: CaO and novel calcium compounds as transesterification catalysts, *Chemical Engineering Research and Design*, 92 (2014) 1519-1530.

- [16] A.K.F. Carvalho, L.R.V. da Conceição, J.P.V. Silva, V.H. Perez, H.F. de Castro, Biodiesel production from *Mucor circinelloides* using ethanol and heteropolyacid in one and two-step transesterification, *Fuel*, 202 (2017) 503-511.
- [17] C.C.A. Loures, M.S. Amaral, P.C.M. Da Rós, S.M.F.E. Zorn, H.F. de Castro, M.B. Silva, Simultaneous esterification and transesterification of microbial oil from *Chlorella minutissima* by acid catalysis route: A comparison between homogeneous and heterogeneous catalysts, *Fuel*, 211 (2018) 261-268.
- [18] M. Farooq, A. Ramli, D. Subbarao, Biodiesel production from waste cooking oil using bifunctional heterogeneous solid catalysts, *Journal of Cleaner Production*, 59 (2013) 131-140.
- [19] N. Mansir, S.H. Teo, U. Rashid, M.I. Saiman, Y.P. Tan, G.A. Alsultan, Y.H. Taufiq-Yap, Modified waste egg shell derived bifunctional catalyst for biodiesel production from high FFA waste cooking oil. A review, *Renewable and Sustainable Energy Reviews*, 82 (2018) 3645-3655.
- [20] P.C.M. Da Rós, C.S.P. Silva, M.E. Silva-Stenico, M.F. Fiore, H.F. de Castro, Microbial Oil Derived from Filamentous Cyanobacterium *Trichormus* sp. as Feedstock to Yield Fatty Acid Ethyl Esters by Enzymatic Synthesis, *Journal of Advances in Biology & Biotechnology*, 12 (2017) 1-14.
- [21] A.B.R. Moreira, V.H. Perez, G.M. Zanin, H.F. de Castro, Biodiesel Synthesis by Enzymatic Transesterification of Palm Oil with Ethanol Using Lipases from Several Sources Immobilized on Silica-PVA Composite, *Energy & Fuels*, 21 (2007) 3689-3694.
- [22] S. Semwal, A.K. Arora, R.P. Badoni, D.K. Tuli, Biodiesel production using heterogeneous catalysts, *Bioresource Technology*, 102 (2011) 2151-2161.

- [23] F.M. da Silva, D.M.M. Pinho, G.P. Houg, I.B.A. Reis, M. Kawamura, M.S.R. Quemel, P.R. Montes, P.A.Z. Suarez, Continuous biodiesel production using a fixed-bed Lewis-based catalytic system, *Chemical Engineering Research and Design*, 92 (2014) 1463-1469.
- [24] S. Furuta, H. Matsushashi, K. Arata, Biodiesel fuel production with solid superacid catalysis in fixed bed reactor under atmospheric pressure, *Catalysis Communications*, 5 (2004) 721-723.
- [25] J. Iglesias, J.A. Melero, L.F. Bautista, G. Morales, R. Sánchez-Vázquez, Continuous production of biodiesel from low grade feedstock in presence of Zr-SBA-15: Catalyst performance and resistance against deactivation, *Catalysis Today*, 234 (2014) 174-181.
- [26] W. Jindapon, P. Kuchonthara, C. Ngamcharussrivichai, Biodiesel production over Ca, Zn, and Al mixed compounds in fixed-bed reactor: Effects of premixing catalyst extrudates with methanol, oil, and fatty acid methyl esters, *Fuel Processing Technology*, 148 (2016) 67-75.
- [27] M. Kim, C. DiMaggio, S.O. Salley, K.Y. Simon Ng, A new generation of zirconia supported metal oxide catalysts for converting low grade renewable feedstocks to biodiesel, *Bioresource Technology*, 118 (2012) 37-42.
- [28] J.A. Melero, L.F. Bautista, J. Iglesias, G. Morales, R. Sánchez-Vázquez, Production of biodiesel from waste cooking oil in a continuous packed bed reactor with an agglomerated Zr-SBA-15/bentonite catalyst, *Applied Catalysis B: Environmental*, 145 (2014) 197-204.
- [29] V. Pugnet, S. Maury, V. Coupard, A. Dandeu, A.-A. Quoineaud, J.-L. Bonneau, D. Tichit, Stability, activity and selectivity study of a zinc aluminate heterogeneous

catalyst for the transesterification of vegetable oil in batch reactor, *Applied Catalysis A: General*, 374 (2010) 71-78.

[30] D.M. Alonso, R. Mariscal, R. Moreno-Tost, M.D.Z. Poves, M.L. Granados, Potassium leaching during triglyceride transesterification using $K/\gamma\text{-Al}_2\text{O}_3$ catalysts, *Catalysis Communications*, 8 (2007) 2074-2080.

[31] S. Baroutian, M.K. Aroua, A.A.A. Raman, N.M.N. Sulaiman, Potassium hydroxide catalyst supported on palm shell activated carbon for transesterification of palm oil, *Fuel Processing Technology*, 91 (2010) 1378-1385.

[32] J.C.T. da Silva, A.D. Gondim, L.P.F.C. Galvão, J.P. da Costa Evangelista, A.S. Araujo, V.J. Fernandes, Thermal stability evaluation of biodiesel derived from sunflower oil obtained through heterogeneous catalysis ($\text{KNO}_3/\text{Al}_2\text{O}_3$) by thermogravimetry, *Journal of Thermal Analysis and Calorimetry*, 119 (2015) 715-720.

[33] O. Ilgen, A.N. Akin, Development of Alumina Supported Alkaline Catalysts Used for Biodiesel Production, *Turk J Chem*, 33 (2009) 281-287.

[34] A. Islam, Y.H. Taufiq-Yap, P. Ravindra, S.H. Teo, S. Sivasangar, E.-S. Chan, Biodiesel synthesis over millimetric $\gamma\text{-Al}_2\text{O}_3/\text{KI}$ catalyst, *Energy*, 89 (2015) 965-973.

[35] X.-f. Li, Y. Zuo, Y. Zhang, Y. Fu, Q.-x. Guo, In situ preparation of K_2CO_3 supported Kraft lignin activated carbon as solid base catalyst for biodiesel production, *Fuel*, 113 (2013) 435-442.

[36] R. Shan, J. Shi, B. Yan, G. Chen, J. Yao, C. Liu, Transesterification of palm oil to fatty acids methyl ester using $\text{K}_2\text{CO}_3/\text{palygorskite}$ catalyst, *Energy Conversion and Management*, 116 (2016) 142-149.

[37] M. Verziu, M. Florea, S. Simon, V. Simon, P. Filip, V.I. Parvulescu, C. Hardacre, Transesterification of vegetable oils on basic large mesoporous alumina supported

alkaline fluorides—Evidences of the nature of the active site and catalytic performances, *Journal of Catalysis*, 263 (2009) 56-66.

[38] E.G. Silveira Junior, E. Simionatto, V.H. Perez, O.R. Justo, N.A.H. Zárata, M.d.C. Vieira, Potential of Virginia-type peanut (*Arachis hypogaea* L.) as feedstock for biodiesel production, *Industrial Crops and Products*, 89 (2016) 448-454.

[39] S. Brunauer, P.H. Emmett, E. Teller, Adsorption of Gases in Multimolecular Layers, *Journal of the American Chemical Society*, 60 (1938) 309-319.

[40] E.P. Barrett, L.G. Joyner, P.P. Halenda, The Determination of Pore Volume and Area Distributions in Porous Substances. I. Computations from Nitrogen Isotherms, *Journal of the American Chemical Society*, 73 (1951) 373-380.

[41] Y. Wang, J.H. Zhu, W.Y. Huang, Synthesis and characterization of potassium-modified alumina superbases., *Physical Chemistry Chemical Physics*, 3 (2001) 2537-2543.

[42] T. Eevera, K. Rajendran, S. Saradha, Biodiesel production process optimization and characterization to assess the suitability of the product for varied environmental conditions, *Renewable Energy*, 34 (2009) 762-765.

[43] F. Ma, M.A. Hanna, Biodiesel production: a review1Journal Series #12109, Agricultural Research Division, Institute of Agriculture and Natural Resources, University of Nebraska–Lincoln.1, *Bioresource Technology*, 70 (1999) 1-15.

[44] M. Taherkhani, S.M. Sadrameli, An improvement and optimization study of biodiesel production from linseed via in-situ transesterification using a co-solvent, *Renewable Energy*, 119 (2018) 787-794.

[45] Y. Alhassan, N. Kumar, I.M. Bugaje, H.S. Pali, P. Kathkar, Co-solvents transesterification of cotton seed oil into biodiesel: Effects of reaction conditions on

quality of fatty acids methyl esters, *Energy Conversion and Management*, 84 (2014) 640-648.

[46] D.P. Luu, N. Takenaka, B.V. Luu, L.N. Pham, K. Imamura, Y. Maeda, Co-solvent method produce biodiesel form waste cooking oil with small pilot plant., *Energy Procedia*, 61 (2014) 2822-2832.

[47] Dianursanti, P. Religia, A. Wijanarko, Utilization of n-Hexane as Co-solvent to Increase Biodiesel Yield on Direct Transesterification Reaction from Marine Microalgae, *Procedia Environmental Sciences*, 23 (2015) 412-420.

[48] X. Liu, X. Xiong, C. Liu, D. Liu, A. Wu, Q. Hu, C. Liu, Preparation of Biodiesel by Transesterification of Rapeseed Oil with Methanol Using Solid Base Catalyst Calcined $K_2CO_3/\gamma-Al_2O_3$, *Journal of the American Oil Chemists' Society*, 87 (2010) 817-823.

[49] W. Cao, H. Han, J. Zhang, Preparation of biodiesel from soybean oil using supercritical methanol and co-solvent, *Fuel*, 84 (2005) 347-351.

[50] W. Xie, H. Li, Alumina-supported potassium iodide as a heterogeneous catalyst for biodiesel production from soybean oil, *Journal of Molecular Catalysis A: Chemical*, 255 (2006) 1-9.

[51] E.C. Abbah, G.I. Nwandikom, C.C. Egwuonwu, N.R. Nwakuba, Effect of Reaction Temperature on the Yield of Biodiesel from Neem Seed Oil., *American Journal of Energy Science*, 3 (2016) 16-20.

[52] J.P.C. Evangelista, T. Chellappa, A.C.F. Coriolano, V.J. Fernandes, L.D. Souza, A.S. Araujo, Synthesis of alumina impregnated with potassium iodide catalyst for biodiesel production from rice bran oil, *Fuel Processing Technology*, 104 (2012) 90-95.

Table 1. Values obtained from tests of mechanical strength of the extruded catalysts with hollow cylindrical shape.

Catalysts	Mechanical strength	
	Length (mm)	Pressure (kgf/cm)
15% K ₂ CO ₃ /85% γ -Al ₂ O ₃	6.98 ± 1.20	1.00 ± .00
25% K ₂ CO ₃ /75% γ -Al ₂ O ₃	6.51 ± 0.70	1.25 ± 0.29
35% K ₂ CO ₃ /65% γ -Al ₂ O ₃	6.86 ± 0.99	2.75 ± 0.61
45% K ₂ CO ₃ /55% γ -Al ₂ O ₃	6.66 ± 1.21	1.67 ± 0.49

Table 2. Specific area, volume and pore size of extruded catalysts with hollow cylindrical shape determined by N₂ adsorption.

Support and catalysts	Textural properties		
	¹ Specific area (m ² /g)	² Pore volume (cm ³ /g)	² Pore size (nm)
γ-alumina	209	0.55	9.8
15% K ₂ CO ₃ / 85% γ-Al ₂ O ₃	114	0.47	14.8
25% K ₂ CO ₃ / 75% γ-Al ₂ O ₃	95	0.42	15.6
35% K ₂ CO ₃ / 65% γ-Al ₂ O ₃	65	0.28	16.1
45% K ₂ CO ₃ / 55% γ-Al ₂ O ₃	64	0.31	17.3

¹BET surface area.

²Average pore volume and size were estimated from BJH model.

Table 3. CO₂ - TPD to measure the basicity and density of basic sites of the extruded catalysts with hollow cylindrical shape.

Catalysts	Desorption temperature of CO ₂ (mmol/g)	CO ₂ desorbed (mmol/g)	Total CO ₂ desorbed (mmol/g)	Total density of basic sites CO ₂ (mmol/m ²)
15% K ₂ CO ₃ /85% γ -Al ₂ O ₃	257.7**	3.16	3.25	0.028
	316.2**	0.093		
25% K ₂ CO ₃ /75% γ -Al ₂ O ₃	367.0**	3.67	3.67	0.038
	258.7**	3.97		
35% K ₂ CO ₃ /65% γ -Al ₂ O ₃	302.9**	0.63	4.60	0.070
	256.6**	2.86	2.86	0.044

Strength of the basic sites: *weak sites: CO₂ desorption between below 160 °C; **medium sites: CO₂ desorption between 160 and 400 °C and *strong sites: CO₂ desorption above 400 °C.**

Table 4. Effect of the molar ratio oil: ethanol on the ethanolic biodiesel production from sunflower oil using 35% K₂CO₃/65% γ -Al₂O₃ extruded catalyst with hollow cylindrical shape. Reaction conditions: 5 wt% catalyst, 200 rpm stirring, 80 °C and 4 h reaction time.

Molar ratio (oil: alcohol)	Biodiesel Yield*		Productivity**	
	(%)		(g/g h)	
	2h	4h	2h	4h
(1:6)	46.66	55.56	0.24	0.14
(1:9)	67.55	72.52	0.35	0.19
(1:12)	97.06	99.28	0.51	0.26

* Yield was defined as the amount of biodiesel formed in relation to the total mass of biodiesel from sunflower oil at specific reaction time.

** Productivity was defined as the mass of biodiesel formed by mass of oil for reaction time (g/g h).

Table 5. Ethanolic biodiesel production with the following reaction parameters: molar ratio of oil: alcohol (1:12), reaction temperature of 80 °C, stirring at 200 rpm and 4 hours of reaction.

Extruded catalysts	Biodiesel yield* (%)		Productivity** (g/g h)	
	2h	4h	2h	4h
15% K ₂ CO ₃ /85% γ -Al ₂ O ₃	58.04±1.2	78.75±7.0	0.305	0.21
25% K ₂ CO ₃ /75% γ -Al ₂ O ₃	65.82±1.3	74.29±11.3	0.345	0.19
35% K ₂ CO ₃ /65% γ -Al ₂ O ₃	97.06±0.6	99.28±0.7	0.515	0.27
45% K ₂ CO ₃ /55% γ -Al ₂ O ₃	87.68±0.2	96.59±3.4	0.46	0.26

* Yield was defined as the amount of biodiesel formed in relation to the total mass of biodiesel from sunflower oil at specific reaction time.

** Productivity was defined as the mass of biodiesel formed by mass of oil for reaction time (g/g h).

Table 6. Studies showing heterogeneous catalysts prepared in different shapes (powder and extrudate).

Catalysts	Catalyst shape	Reaction parameters			Biodiesel yield (%)	Number of cycles	References
		Oil: alcohol (molar ratio)/catalyst mass (wt %)	Temperature (°C)/ reaction time (min)/ stirring (rpm)				
K_2CO_3 /palygorskite	Powder	Palm: methanol (1: 12)/5	65/210/800		8	[36]	
ZSAH-400 (Ca, Zn, and Al mixed and 400°C calcination)	Powder and Extrudate: Rods (2mm)	Palm: methanol (1: 30)/135mL	65/ 480/Fixed bed reactor	96.5	--	[26]	
$\gamma-Al_2O_3/KI$	Spherical millimetric particles	Palm: methanol (1:14)/8	65/90/800	96.4	11	[34]	
KNO_3/Al_2O_3	Powder	Sunflower: ethanol (1:15)/2-8	--/480/--	60.0	--	[32]	
$(Al_2O_3)_{8.2}(ZnO)_{2.0}$	Pellets	Soybean: methanol and ethanol (1:10)	100/300/ fixed bed tubular reactor	75.0 35.0	Active for 120h	[23]	
Zr-SBA-15/bentonite	uniform rods (1.5 mm)	Waste cooking oil: methanol (1:50)/28g	210/30/70bar packed bed reactor	96.0	260 h	[28]	
Zr-SBA-15	uniform rods (1.0 mm)	Animal Fat and Waste cooking Methanol (1:50)/12.45	209/360/2000	92.0	3	[25]	
K_2CO_3 supported on lignin Kraft	Powder	Rapeseed: methanol (1:5)/3	65/120/--	97.6	4	[35]	

ZnO–TiO ₂ –Nd ₂ O ₃ /ZrO ₂ and ZnO–SiO ₂ – Yb ₂ O ₃ /ZrO ₂	cylindrical pellets	Feed mixture of 67% soybean and 33% FFA: methanol (1:9.4)	195/44/300psi tubular reactor	99.0	Active up to 6 months	[27]
KI/Al ₂ O ₃	Powder	Rice bran oil: methanol (1:15)/5	--/480/--	95.2	--	[52]
Zinc aluminate	Pellets (2 mm and 3–5 mm)	Rapeseed: methanol (1: 27)/4	200/360/800	70.0	3	[29]
KOH/AC (Activate carbon)	Powder	Palm: methanol (1:24)/10	64/60/--	98.0	3	[31]
KF/Al ₂ O ₃	Powder	Sunflower, rapeseed and soybean: methanol (1:4)/ 300 mg	70/180/--	96.0	4	[37]
WO ₃ /ZrO ₂ , SO ₄ /SnO ₂ and SO ₄ /ZrO ₂	Cylindrical pellets	Soybean: methanol (1:40)/4g and n- octanoic acid: methanol (1:4.5)/4g	200–300 and 175-200/ 1200	90.0 100.0	Activity up to 100h	[24]
K ₂ CO ₃ /γ-Al ₂ O ₃	Hollow cylinder (5mm and 2mm)	Sunflower: ethanol (1:12)/5	78/120/200	97.0	2	In this study
				100.0	4	

Table 7. Physicochemical properties of produced ethanolic biodiesel from sunflower oil by transesterification using extruded catalyst with hollow cylindrical shape.

Properties	Standard*		Biodiesel produced
	Methods	*Limits	
Density (20 °C, kg/m ³)	ASTM D1298	850 - 900	864 ±5.0
Kinematic viscosity (40 °C, mm ² /s)	ASTM D445	3.0 - 6.0	4.9 ±0.3
Acid number (mg NaOH/g)	ASTM D664	0.50 (max.)	0.36 ±0.1
Iodine value (g I ₂ /100g)	EN 14111	130 (max.)	123.1 ±1.5

*Brazilian biodiesel standards ANP (*National Agency of Petroleum, Natural Gas and Biofuels*).

Figure captions

Fig 1. Thermogravimetric analysis (TGA - DTG) for: a) boehmite and b) K_2CO_3 .

Fig 2. X-ray diffraction patterns of the catalysts with different mass ratio of K_2CO_3 (15, 25, 35 and 45%) impregnated into γ - Al_2O_3 extruded support.

Fig 3. Micrographs (SEM) of the catalysts with composition of 35% K_2CO_3 /65% γ - Al_2O_3 .

Fig 4. Ethanolic sunflower biodiesel production as a function of molar ratio oil: alcohol. Symbols: ■ 1:6; ● 1:9; ▲ 1:12. Reaction conditions: 5 wt% mass of extruded catalyst (35% K_2CO_3 /65% γ - Al_2O_3) at 80 °C, 200 rpm and 4 h reaction time.

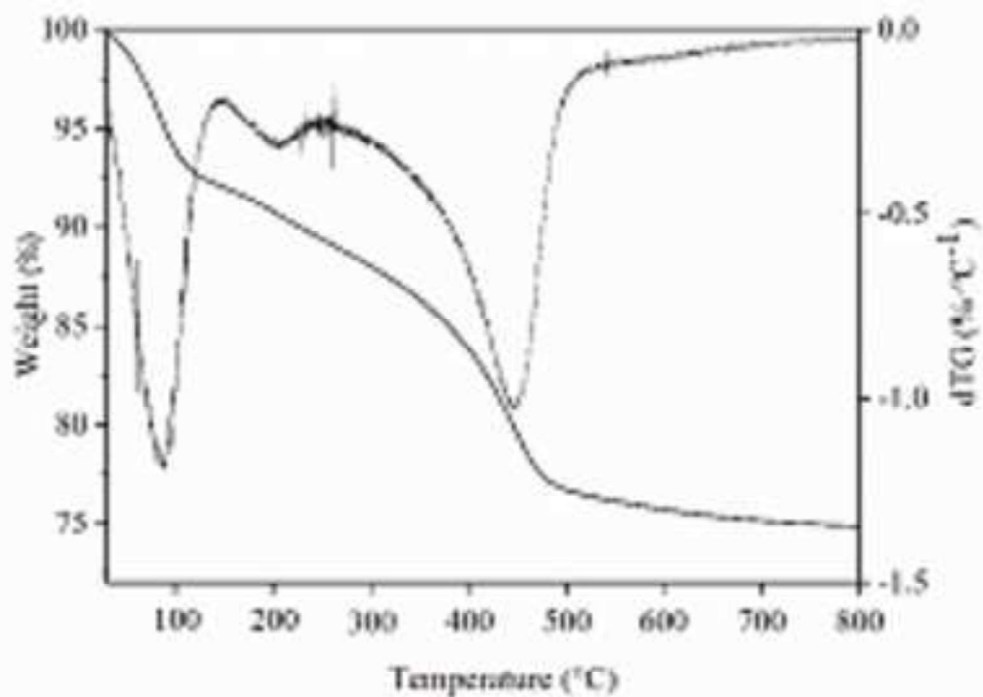
Fig 5. Ethanolic sunflower biodiesel production using K_2CO_3 catalyst (■ 15%, ● 25%, ▲ 35%, ▼ 45%) impregnated on the γ - Al_2O_3 support. Reaction conditions: oil: ethanol molar ratio 1:12, catalyst amount, 5 wt% at 80 °C and 4 h reaction time.

Fig 6. Ethanolic sunflower biodiesel production using 35% K_2CO_3 /65% γ - Al_2O_3 catalyst prepared in different forms: ● active phase impregnated on the cylinder hollow extruded support; ■ active phase impregnated on the solid cylinder extruded support ▲ active phase impregnated on powder. Reaction conditions were: oil: alcohol molar ratio 1:12, catalyst amount 5 wt%, 200 rpm, 4 h reaction and temperature of the 80 °C.

Fig 7. Ethanolic sunflower biodiesel production using 35% K_2CO_3 /65% γ - Al_2O_3 extruded catalyst with molar ration conditions of oil: alcohol of the (1:12), catalyst amount 5 wt%, 2 h reaction and temperature conditions: ■ 80 °C; ● 70 °C; and ▲ 60 °C.

Figure 1
[Click here to download high resolution image](#)

a)



b)

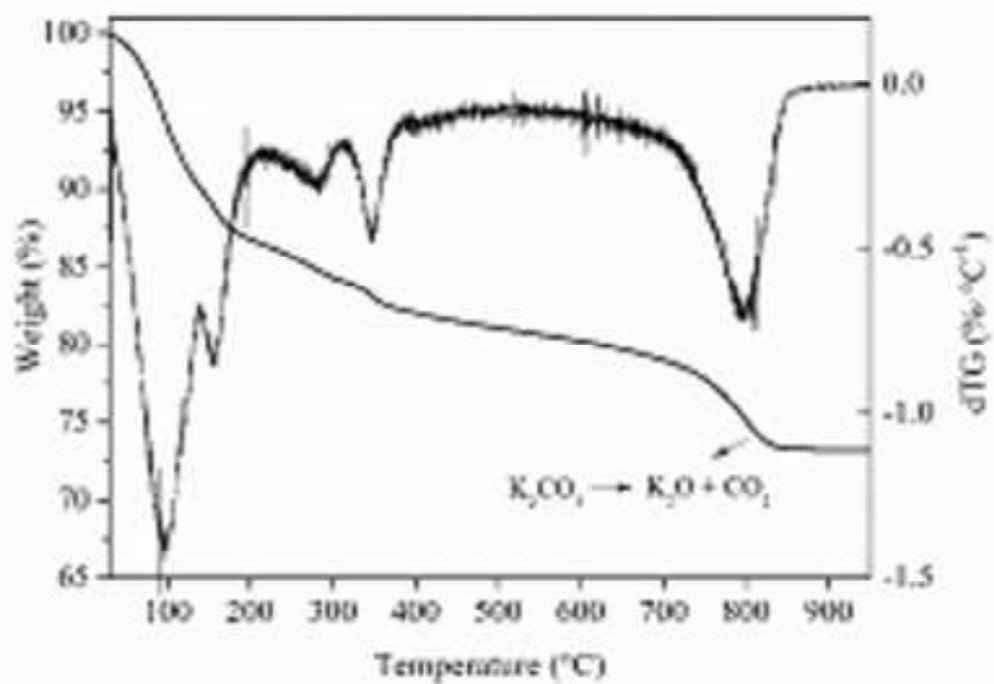


Figure 2
[Click here to download high resolution image](#)

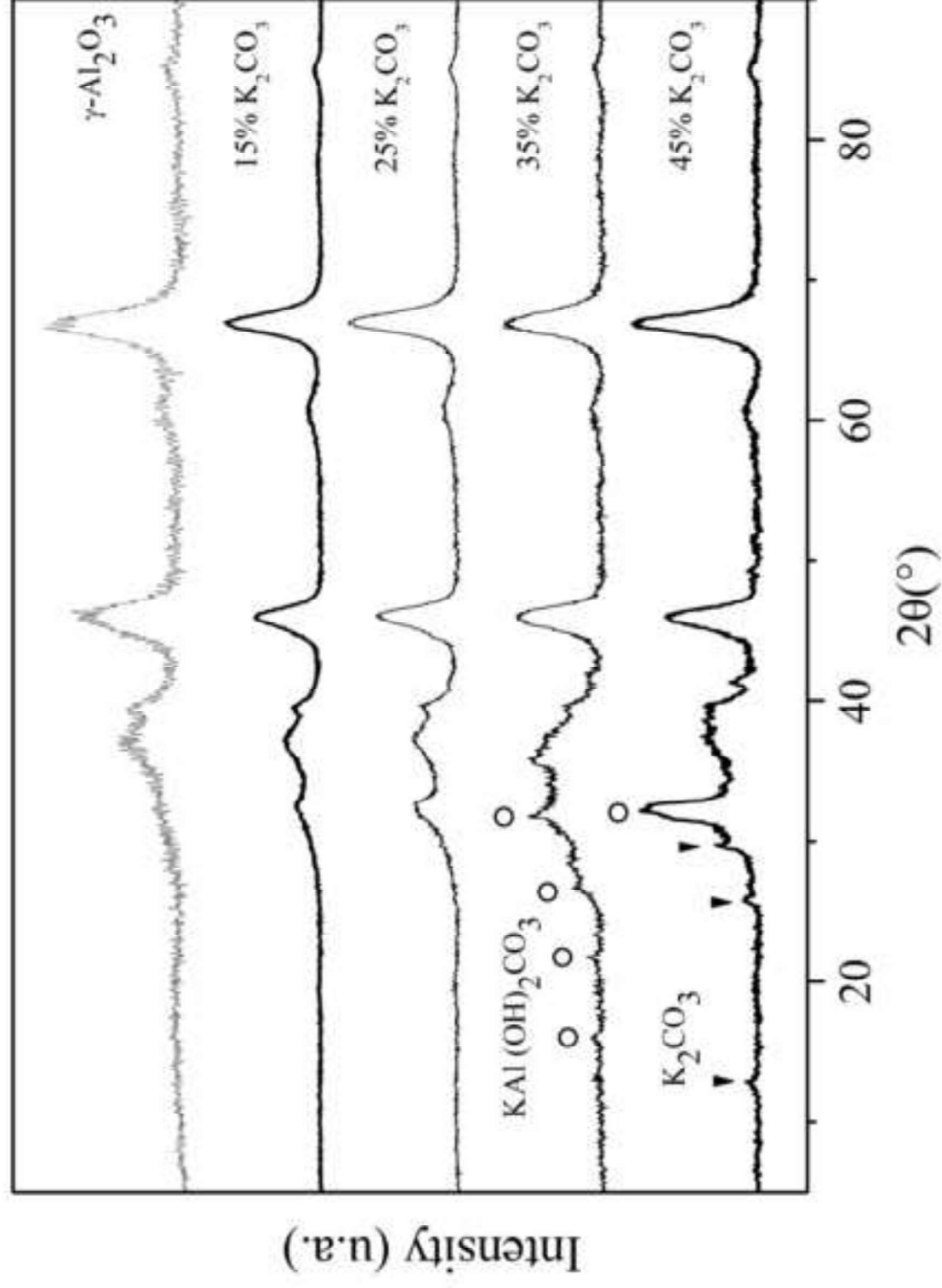
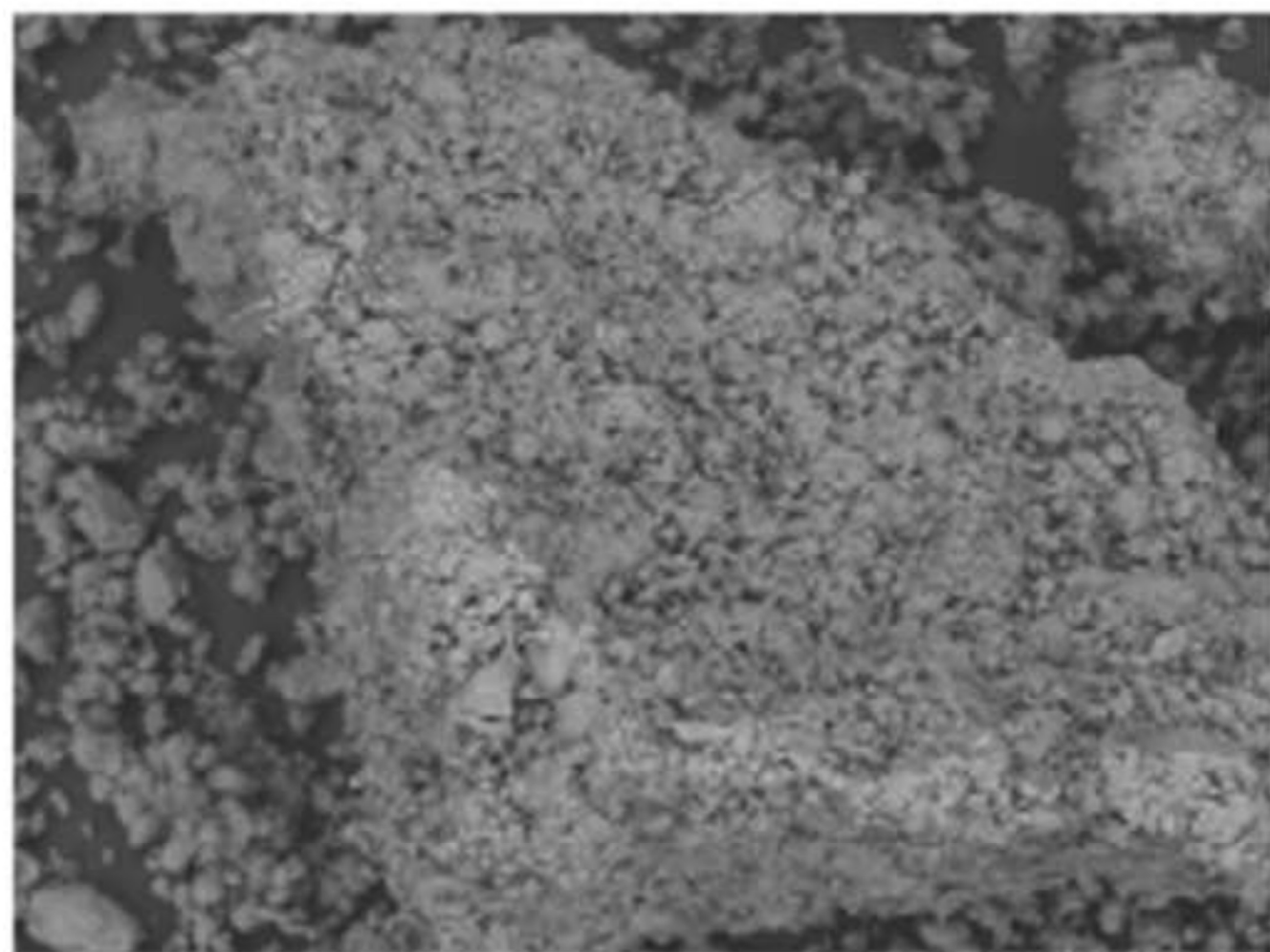


Figure 3
[Click here to download high resolution image](#)



35K2M C.O

x250 300 um

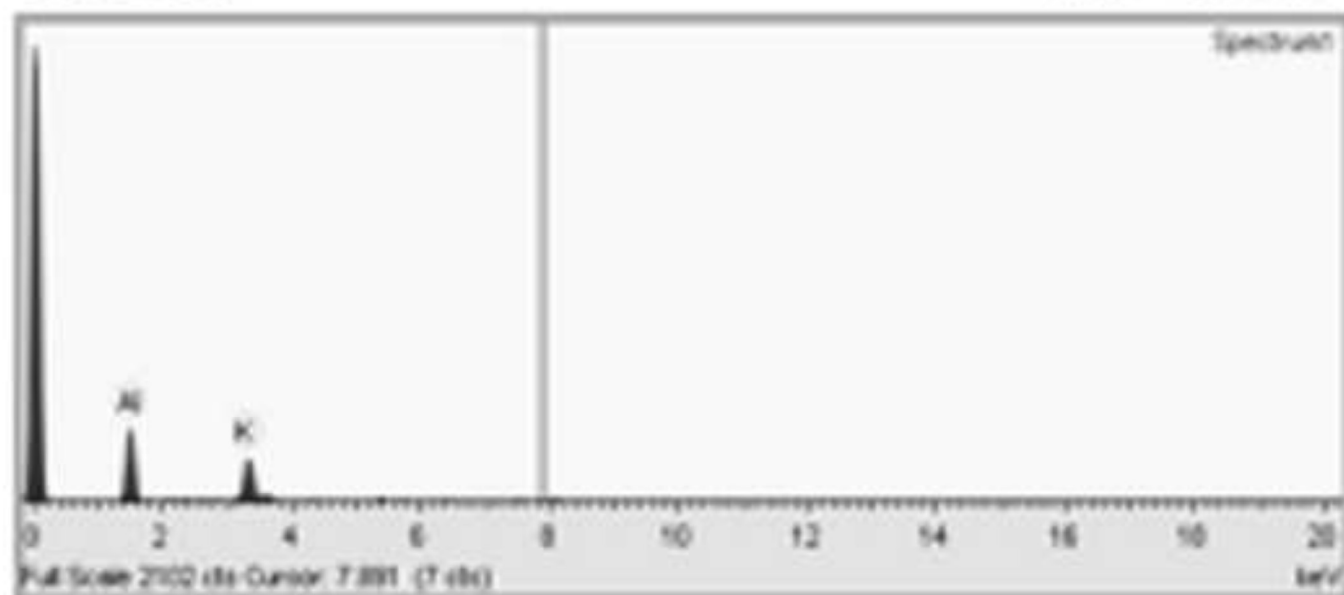


Figure 4
[Click here to download high resolution image](#)

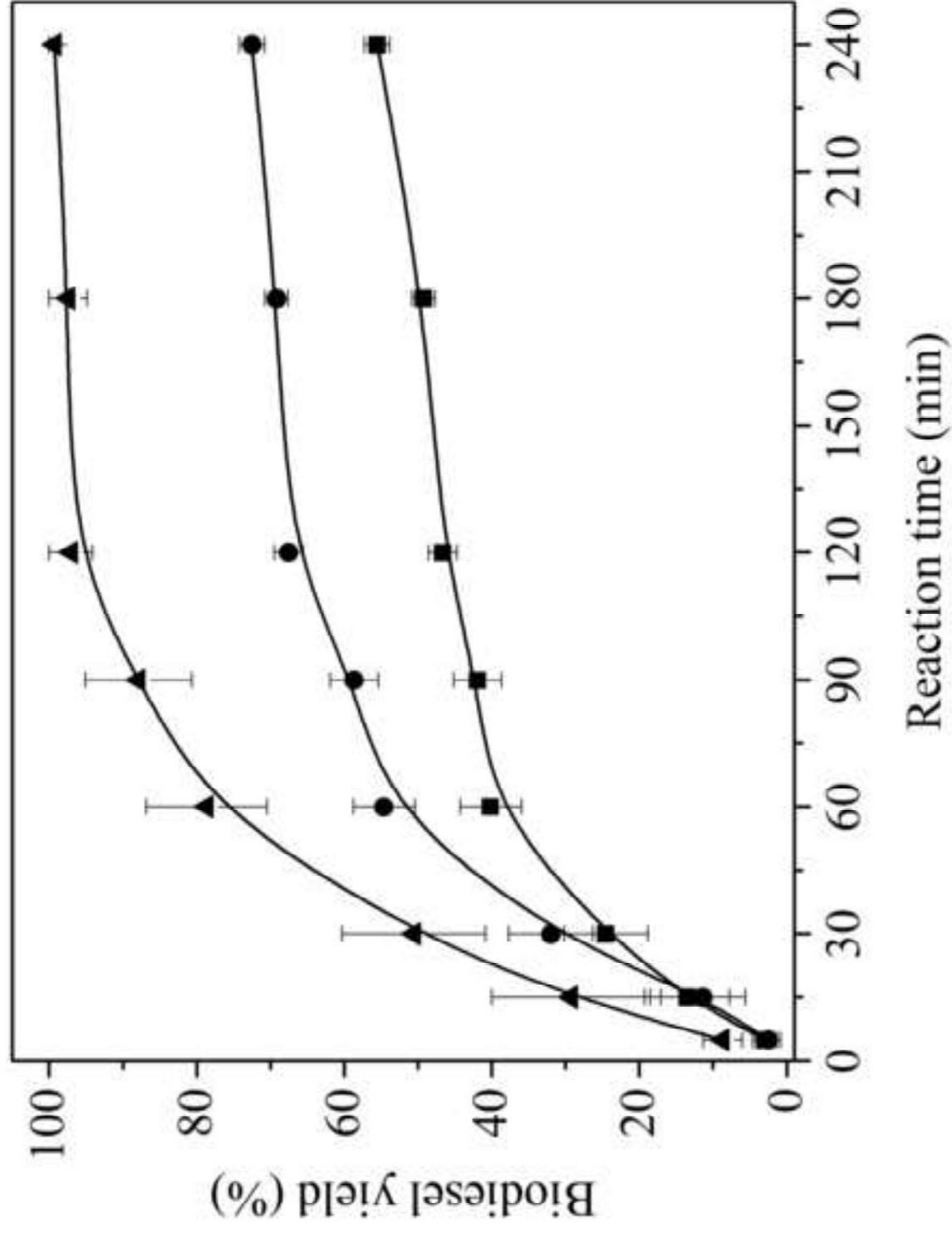


Figure 5
[Click here to download high resolution image](#)

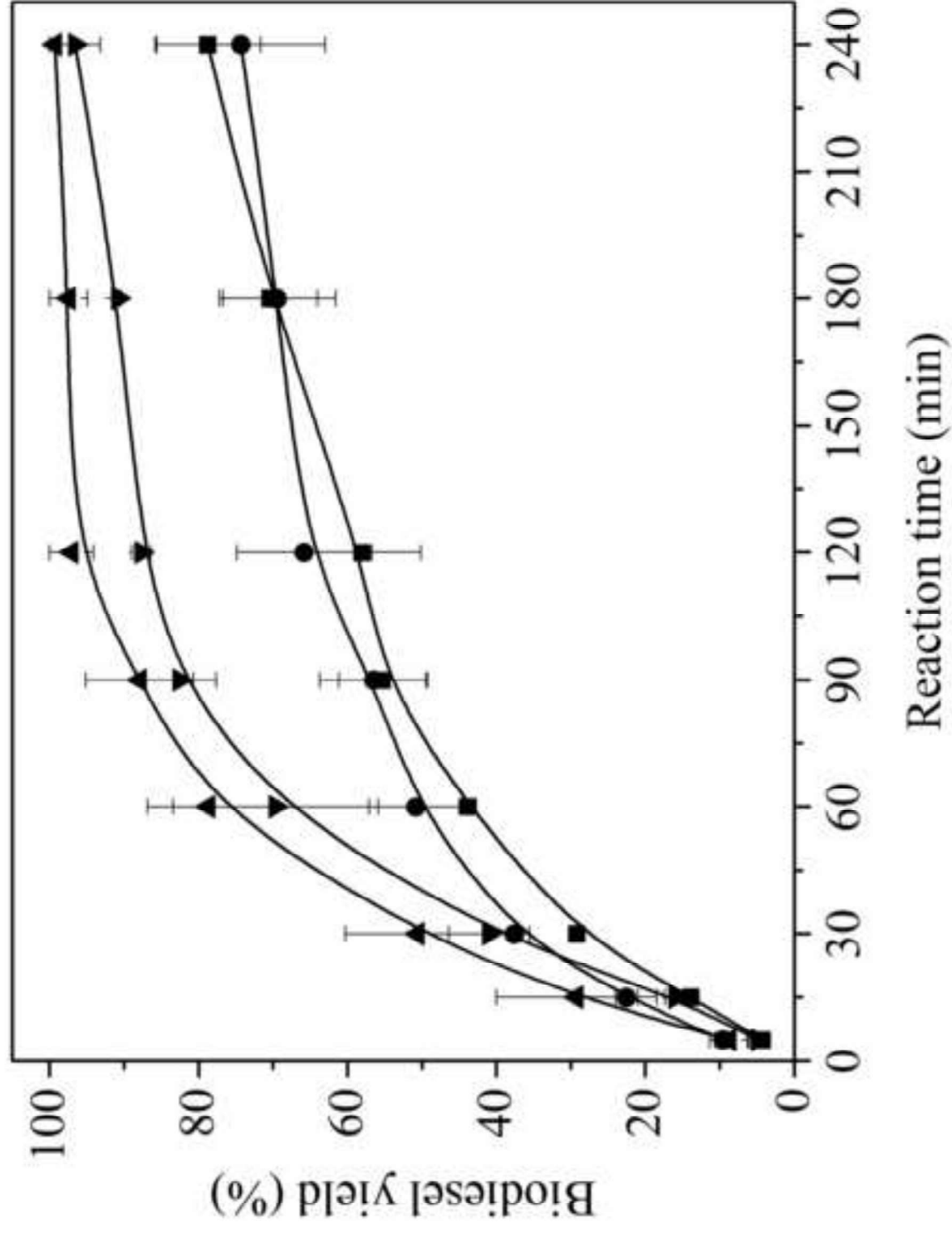


Figure 6
[Click here to download high resolution image](#)

